

Magnetic response of split ring resonators (SRRs) at visible frequencies

Basudev Lahiri¹, Scott G. McMeekin², Ali Z. Khokhar¹, Richard M. De La Rue¹ and Nigel P. Johnson^{1*}

¹ Department of Electronics and Electrical Engineering, University of Glasgow, Glasgow, G12 8LT, UK

² School of Computing and Engineering, Glasgow Caledonian University, Glasgow, G4 0BA, UK

* njohnson@elec.gla.ac.uk

Abstract: In this paper, we report on a substantial shift in the response of arrays of similarly sized Split Ring Resonators (SRRs), having a rectangular U-shaped form - and made respectively of aluminium and of gold. We also demonstrate that it is possible to obtain the polarization dependent LC peak in the visible spectrum - by using SRRs based on aluminium, rather than gold. The response of metallic SRRs scales linearly with size. At optical frequencies, metals stop behaving like nearly perfect conductors and begin displaying characteristically different behaviour, in accord with the Drude model. The response at higher frequencies, such as those in the visible and near infra-red, depends both on their size and on the individual properties of the metals used. A higher frequency limit has been observed in the polarization dependent response (in particular the LC resonance peak) of gold based SRRs in the near infrared region. By using aluminium based SRRs instead of gold, the higher frequency limit of the LC resonance can be further shifted into the visible spectrum.

© 2010 Optical Society of America

OCIS codes: (160.3918) Metamaterials; (160.4236) Nanomaterials; (160.4670) Optical materials; (160.4760) Optical properties; (160.3820) Magneto-optical materials; (220.4241) Nanostructure fabrication; (140.4780) Optical resonators; (250.0250) Optoelectronics; (250.5403) Plasmonics; (160.6000) Semiconductor materials; (160.6030) Silica; (240.6490) Spectroscopy; surface.

References and links

1. V. G. Veselago, "The electrodynamics of substances with simultaneously negative values of ϵ and μ ," *Sov. Phys.* **10**(4), 509–514 (1968).
2. J. B. Pendry, A. J. Holden, D. J. Robbins, and W. J. Stewart, "Magnetism from conductors and enhanced Non-Linear Phenomena," *IEEE Trans. Microw. Theory Tech.* **47**(11), 2075–2084 (1999).
3. S. Linden, C. Enkrich, M. Wegener, J. Zhou, T. Koschny, and C. M. Soukoulis, "Magnetic Response of Metamaterials at 100 THz," *Science* **306**(5700), 1351–1361 (2004).
4. V. M. Shalaev, "Optical negative index metamaterials," *Nat. Photonics* **1**(1), 41–48 (2007).
5. S. Linden, C. Enkrich, G. Dolling, M. W. Klein, J. Zhou, T. Koschny, C. M. Soukoulis, S. Burger, F. Schmidt, and M. Wegener, "Photonic Metamaterials: Magnetism at Optical Frequencies," *IEEE J. Sel. Top. Quantum Electron.* **12**(6), 1097–1105 (2006).
6. C. Rockstuhl, F. Lederer, C. Etrich, T. Zentgraf, J. Kuhl, and H. Giessen, "On the reinterpretation of resonances in split-ring-resonators at normal incidence," *Opt. Express* **14**(19), 8827–8836 (2006).
7. J. Zhou, T. Koschny, M. Kafesaki, E. N. Economu, J. B. Pendry, and C. M. Soukoulis, "Saturation of the magnetic response of split ring resonators at Optical frequencies," *Phys. Rev. Lett.* **95**(22), 1–4 (2005).
8. M. W. Klein, C. Enkrich, M. Wegener, C. M. Soukoulis, and S. Linden, "Single-slit split-ring resonators at optical frequencies: limits of size scaling," *Opt. Lett.* **31**(9), 1259–1261 (2006).
9. S. Tretyakov, "On geometrical scaling of split-ring and double bar resonators at optical frequencies," *Metamaterials (Amst.)* **1**(1), 40–43 (2007).
10. <http://www.rsoftdesign.com/products.php?sub=Component+Design&itm=FullWAVE>. 2nd December 2009.
11. W. J. Padilla, A. J. Taylor, C. Highstre, M. Lee, and R. D. Averitt, "Dynamic Electric and Magnetic Metamaterial Response at Terahertz Frequencies," *Phys. Rev. Lett.* **96**(10), 1–4 (2006).
12. H.-T. Chen, W. J. Padilla, J. M. O. Zide, S. R. Bank, A. C. Gossard, A. J. Taylor, and R. D. Averitt, "Ultrafast optical switching of terahertz metamaterials fabricated on ErAs/GaAs nanoisland superlattices," *Opt. Lett.* **32**(12), 1620–1622 (2007).

13. N. P. Johnson, A. Z. Khokhar, H. M. H. Chong, R. M. De La Rue, and S. McMeekin, "Characterisation at infrared wavelengths of metamaterials formed by thin-film metallic split-ring resonator arrays on silicon," *Electron. Lett.* **42**(19), 1117–1119 (2006).
14. I. El-Kady, M. M. Sigalas, R. Biswas, K. M. Ho, and C. M. Soukoulis, "Metallic Photonic crystals at optical wavelengths," *Phys. Rev.* **62**, 15299 (2000).
15. P. Marcos, and C. M. Soukoulis, "Transmission studies of left-handed materials," *Phys. Rev. B* **65**(033401), 1–4 (2001).
16. Z. Sheng, and V. V. Varadan, "Tuning the effective properties of metamaterials by changing the substrate properties," *J. Appl. Phys.* **101**(1), 4–7 (2007).

1. Introduction

Metamaterials exhibit electromagnetic effects, such as negative refractive index [1], that are not readily available in naturally occurring materials. They are often fabricated as periodic arrays of metallic microstructures that are individually smaller than the wavelength of radiation in the region of interest. These structures replace the atoms and molecules of conventional materials - and determine the overall electromagnetic response of the material. The oscillation of the electrons in the microstructures of the metamaterial gives rise to specific electromagnetic responses [2]. By adjusting the geometries of the constituent microstructures, a customized electromagnetic response can be obtained. The "U" shaped split-ring resonators (SRR) is arguably the most common element used in forming the basic microstructure of metamaterials. SRRs can be considered, in their fundamental resonance, as behaving like an LC oscillatory circuit that contains a single turn magnetic coil of inductance - in series with a capacitance produced by the gap between the arms of the SRR. For normal incidence with TE polarization mode, when the incident electric field is across the gap, the electric field couples with the capacitance of the SRR and generates a circulating current around it. This circulating current induces a magnetic field in the bottom or horizontal arm of the SRR and also interacts with the external field to generate the magnetic resonance identified as an LC resonance by Linden et al. [3]. When the incident light TM polarized, the electric field cannot couple to the capacitance of the SRR and therefore generates only electric (plasmon) resonances [2–4]. The LC resonance of the SRR is given as $\omega_{LC} = 1/\sqrt{LC}$ and is inversely proportional to the size (dimension) of SRRs [5]. Figure 1 shows the optimized unit cell of an SRR array for the measurement arrangements with two different polarizations that are clearly distinct for normally incident light.

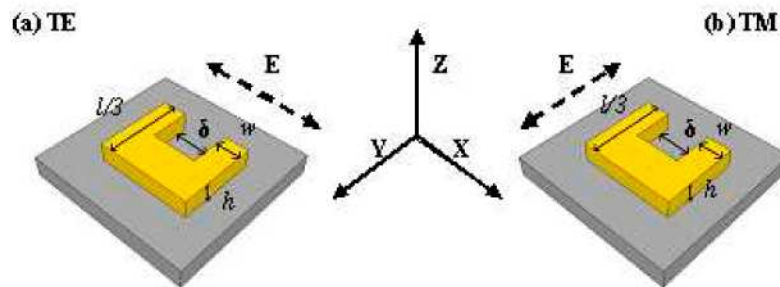


Fig. 1. A single unit cell of the SRR array, with l being the overall length, w is the width of arm, h the thickness (height) of SRR - and δ the gap between arms. All measurements were performed normal (parallel to Z axis) to the surface and with: (a) TE measurements having the Electric field (dashed line) parallel to the SRR arms (parallel to the X-axis) and (b) TM measurements having the Electric field perpendicular to the SRR arms (parallel to Y-axis). In all our experiments the thickness (h) is kept constant at 50 nm.

There has been a considerable effort to scale the sizes of SRRs to nanometer levels - and push the LC resonance to higher frequencies. Rockstuhl et al. [6] have examined the various resonances of specifically rectangular U-shaped SRRs and identify all the resonances predicted and observed as plasmonic resonances. The interpretation of the behaviour of the

SRRs, formed in arrays, was based primarily on their dimensions - and the detailed properties of the metal were not examined closely.

It has previously been found that the magnetic response of the “rectangular C” shaped SRR structures typically saturates just before the visible region is reached - and cannot be shifted indefinitely to higher frequencies by reducing the size of the SRRs [7,8]. Tretyakov has studied this phenomenon in the scaling of SRRs and the saturation of the frequency response, using an LC equivalent circuit model [9]. This model considers the dependence of the achievable resonant frequency on the geometric shape of the SRR, as well as arguing for the involvement of an additional kinetic inductance term and an additional distributed capacitance term.

In this paper we shall refer to the model of Tretyakov in order to help explain some of the results that we have obtained. In the present work, we investigate the differences that occur in the responses of SRRs with nominally identical dimensions - but made up alternatively of aluminium and gold. We report observation of a substantial shift in response between the aluminium and gold SRRs. Furthermore, we utilize this shift to bypass the resonance saturation behaviour of gold (and, by implication, silver) SRRs - and demonstrate a polarization dependent LC resonance peak at visible wavelengths for the aluminium based SRRs.

The changes in the properties of metals at higher frequencies, where the metal properties behave according to the Drude model and both the real and the imaginary parts of the dielectric function must be considered, have so far not been fully explored in relation to the high-frequency resonance saturation behaviour of the SRRs [3,7,8]. The “rectangular C” shaped structure studied by Zhou et al. [7] and Tretyakov [9] suffers from extra capacitance, due to the presence of additional pieces at the ends of the arms and giving a reduced SRR gap dimension, thereby decreasing the resonance frequency. By reducing the total capacitance, the “four gap” structure proposed by Zhou et al. [7], ‘in principle’, can give a higher resonant frequency, comparable with that achieved in our experiment. But the “four gap” structure requires extremely small overall dimensions (~35 nm) and presents a very severe fabrication challenge. Here we have shown that, with suitably reduced arms, “rectangular U” shaped SRRs can give LC resonance at wavelengths down to 530 nm, thus demonstrating the advantage of this geometry.

2. Fabrication and measurement

The SRR patterns were transferred on to either medium-doped silicon or fused silica substrates using electron beam lithography (EBL). A bi-layer of PMMA resist of ~100 nm thickness for each layer was spun over the substrates - and, in the case of silica, a thin aluminium charge dissipation layer was deposited on top of the resist. After development the patterns were either subjected to an electron beam deposition process of 2 nm titanium for adhesion and then 48 nm of gold for the gold SRRs, or 50 nm of aluminium was deposited directly for the aluminium samples. The patterns were written as square arrays over an area of approximately 300 μm x 300 μm . In total eleven different sized SRRs ($l/3$ varying from ~1000 nm to ~100 nm) made up of gold and aluminium fabricated over both silicon and silica substrates were measured. The reflectance measurements were always performed at normal incidence with an optical microscope, using a X10 lens with an NA of 0.25, a white light source - and a monochromator with either an InGaAs detector (for operating range: 0.8 μm – 1.6 μm) or a SiGe detector (for operating range 0.4 μm to 0.8 μm) and lock-in amplifier. The polarization control in this case was obtained by rotating the samples by 90° with respect to a linear polarized beam, to obtain two different sets of polarization dependent data. For the measurements at longer wavelengths (in the range from 1 μm to 3 μm), measurements were taken at normal incidence with a BioRad FTS 60 FTIR spectrometer equipped with a Cassegrain microscope. The FTIR beam was polarized using a KRS5 polarizer adapted to the appropriate wavelength region. A diaphragm was used to restrict the entire incident light beam to a spot size of ~250 μm X 250 μm in area. For reflectance measurements at higher wavelengths (in the range from 2.5 μm to 15 μm), we have used a Nicolet Continuum 6700

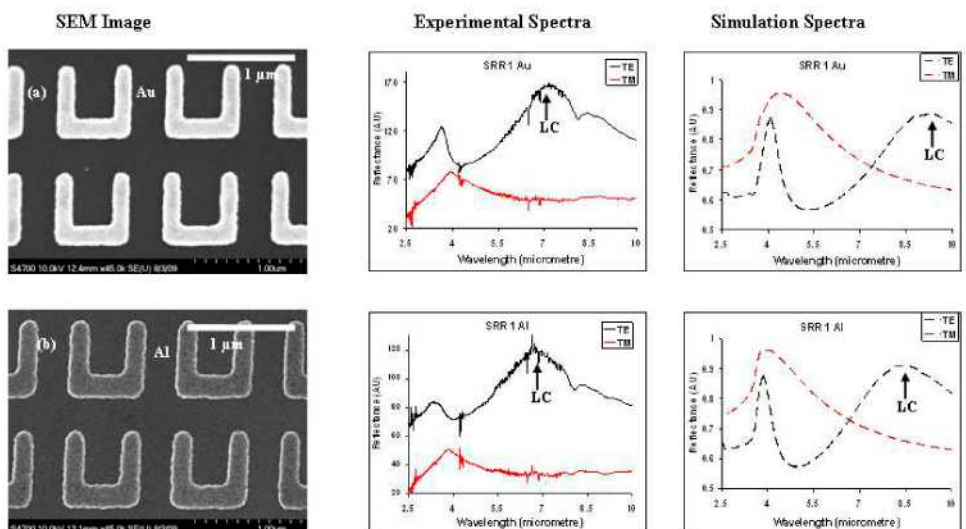
FTIR spectrometer equipped with an IR microscope. A nitrogen-cooled mercury-cadmium-telluride (CMT) detector was used in these measurements. All measurements were performed at normal incidence. This FTIR beam was polarized using a Continuum ZnSe IR polarizer. The reflectance measurements were normalized with respect to the reflectance of the bare silicon substrate, after each measurement, for the silicon samples - and to a gold mirror for silica substrates - and were taken for two orthogonal linear polarizations of incident light oriented simultaneously with respect to the array axes and the SRR element orientation.

3. Results and discussions

The modeling of the structures was performed using Fullwave, a commercial FDTD simulation package from RSoft. A unit cell was defined with dimensions equal to the spacing of the SRR array with the SRR structure centered within the cell. The boundary conditions for the cell were set as periodic in the coordinates perpendicular to the propagation direction, effectively extending the array to infinity - and as a perfectly matched layer (PML) in the direction of propagation, to eliminate any reflections from the boundaries. The dimensions of the SRR structure and the array used in the simulation were obtained from SEM measurements of the experimental structures, in order to minimize errors due to fabrication tolerances. The grid size for the FDTD simulation was set at an eighth of the minimum feature size in each direction. The frequency dependent complex dielectric properties of the Al, Au, Si and SiO₂ constituent materials were based upon the material parameters defined within the Fullwave software. The Al and Au layers were modeled using a Lorentz-Drude model, the SiO₂ substrate was modeled using a Lorentz model and the Si substrate model was based on experimental material parameters measured across the wavelength range of interest [10].

One approach for the potential application of SRRs in optical switching and tunability is to fabricate them on active substrates such as medium-doped silicon, the properties of which can be changed by external means [11,12]. Figure 2 shows various, nominally similar, SRRs made of gold and aluminium, fabricated on silicon substrates - and their corresponding reflection spectra.

Large Au and Al SRRs on Silicon Substrate



Small Au and Al SRRs on Silicon Substrate

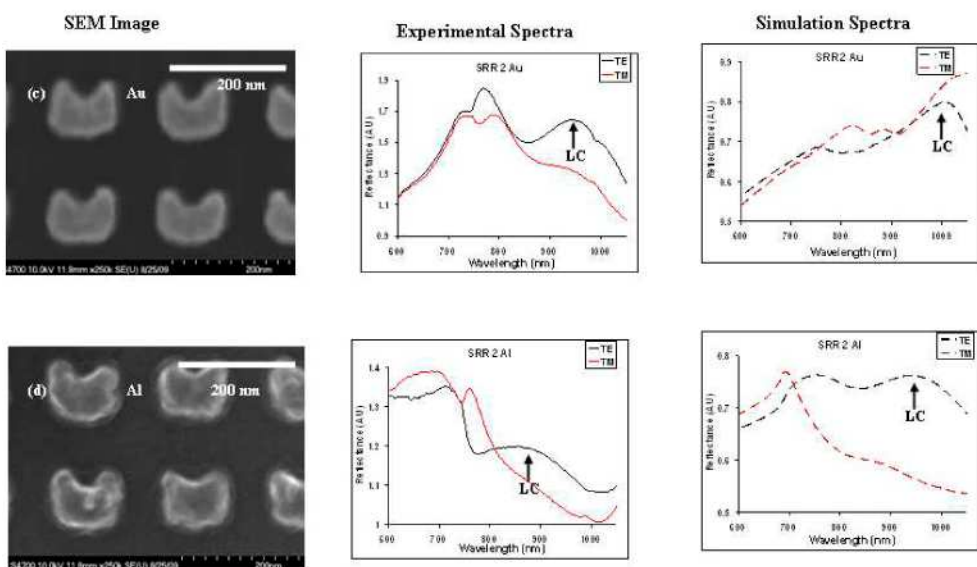


Fig. 2. Table showing the reflectance spectra of the different SRR patterns fabricated on silicon. The first two rows are 'large' (~800 nm) SRRs with: (a) SRR 1 Au and (b) SRR 1 Al. The last two rows are 'small' (~150 nm) SRRs with: (c) SRR 2 Au and (d) SRR 2 Al, along with their corresponding experimental (solid curves) and simulation (dashed) spectra. The black curves (solid and dashed) are for TE polarisation - and the red curves (solid and dashed) are for TM polarisation measurements.

In Fig. 3, we compare the position of magnetic resonance (LC peaks) of nominally identical Al and Au SRRs fabricated on silicon.

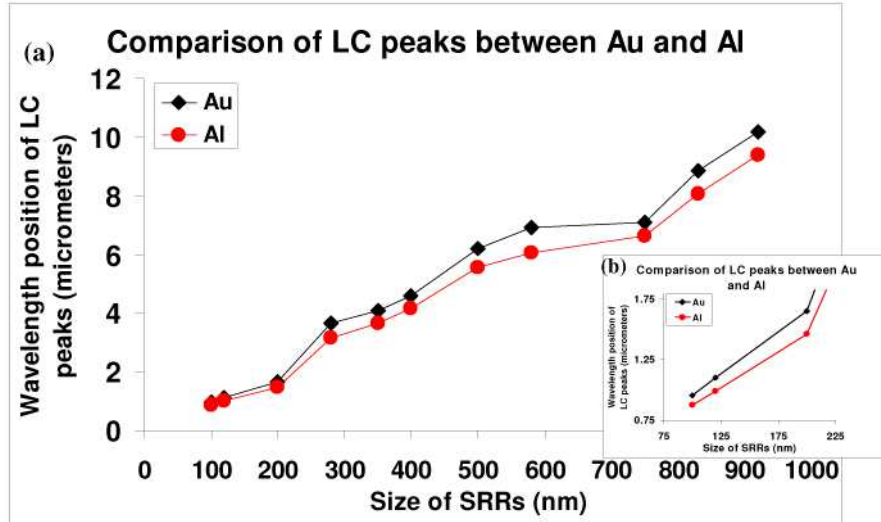


Fig. 3. (a) LC peak positions of Al and Au SRRs fabricated on silicon. (b) Inset comparing the position of LC peaks for Al and Au SRRs of size ~200 to 75 nm

Figure 2 and Fig. 3. shows that, for larger SRRs (with length dimensions in the range from ~1000 nm to 500 nm), the difference between the wavelengths of the Al and Au resonances is approximately 400 nm - but, as the size of the SRRs starts to reduce (below 300nm), the difference between the resonance positions also starts to shrink - and, for SRRs of size ~100 nm, the difference between the Al and Au resonance positions becomes less than 200 nm. This reduction in the difference can be attributed to the saturation of the SRR resonances at higher frequencies [7,8]. From low frequencies up to several Terahertz, the magnetic resonance (LC resonance) scales reciprocally with the dimensions of the SRRs. However, at higher frequencies, the resonance of the SRRs no longer shifts to higher frequencies as the SRRs are reduced in size. At these higher frequencies (in the visible and near infrared regimes) the kinetic energy of the electrons in the metal becomes a dominant feature, which in turn limits the circulating electric current produced by the coupling of the SRR arms, in turn limiting its LC response [7,8].

In addition, at resonance wavelengths below the electronic band-gap of silicon (i.e. below 1.1 μm), illuminating the SRRs excites hole-electron pairs in the substrate - and thereby potentially reduces the magnitude of the resonances of both the LC and plasmonic peaks. We believe this effect to be the main reason for the diminished amplitudes of the resonances for the small sized SRRs on silicon, as compared with those for their larger counterparts.

Overall, apart from the broadening of the LC feature and the possible reduction in the LC resonance magnitude associated with aluminium, the differences between the spectra are not large. However the size of the total inductance (as proposed by Tretyakov [9]) that should be added while reinterpreting such structures at higher frequencies (and as also previously interpreted by Zhou et al [7]) is due to the additional kinetic inertia associated with the motion of the electrons, which depends on the choice of metal. According to the Tretyakov model [9], if the total length of the SRR is l , the width of its arm is w and the thickness (height) of the SRR is h and δ is the gap between the SRR arms (as shown in Fig. 1.) and assuming uniform current density over the cross section of the SRR, the resonant frequency of the SRR is given by:

$$\omega_0 = \frac{1}{\sqrt{(L + L_{add})(C + C_{add})}} \quad (1)$$

Where the additional capacitance and inductance are given by:

$$C_{add} = \frac{\epsilon_0 \epsilon_r wh}{l_{eff}} \text{ and } L_{add} = \frac{l_{eff}}{\epsilon_0 wh \omega_p^2} \quad (2)$$

Where l_{eff} is the effective conductor length that Tretyakov [9] assumes to be $l_{eff} = (\pi/2)l$ and ω_p is the Plasma frequency.

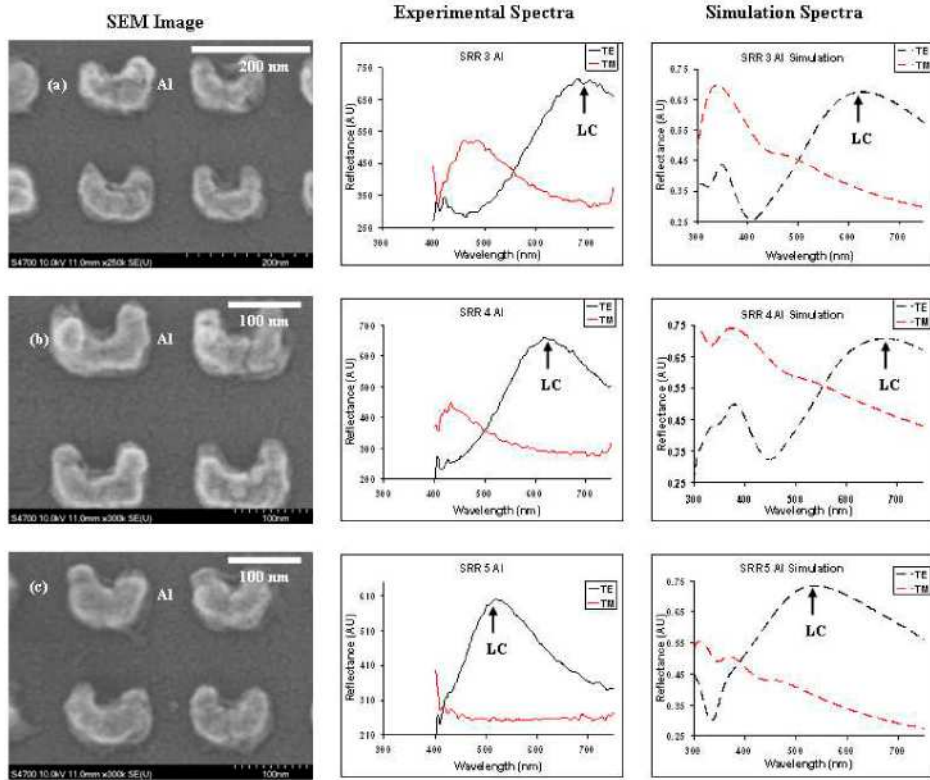
The additional inductance term, L_{add} , associated with the kinetic energy of the electrons depends strongly on the plasma resonance frequency and therefore on the choice of metal. This has been shown in our previous work [13] where similar sized aluminium based SRRs showed LC resonance at higher frequencies than their equivalent gold counterparts. At frequencies below the Plasma frequency, it is the strongly plasma-frequency dependent term for the kinetic inductance that plays a crucial role. Equation (2) indicates that this additional inductance is inversely proportional to the square of the plasma frequency of the metal. The plasma frequency of the metal is equal to 3750 THz for aluminium and 2175 THz for gold [14]. The higher plasma frequency of aluminium will result in a lower additional inductance (L_{add}) and therefore in a shorter resonance wavelength.

The reduction in the magnitude of the reflection resonance for aluminium SRRs can be attributed to the difference in the damping frequency of the metals. In the Drude model, the damping (collision) frequency is associated with absorption and losses. The damping frequency of aluminium is 19.4 THz and that of gold is 6.5 THz [14]. A metal having higher values of damping frequency tends to be more absorptive and lossy. Since aluminium has a higher damping frequency than gold, it is more absorptive and hence the magnitude of the response of an array of aluminium SRRs is lower than that of gold.

Apart from their physical size, the frequency of the LC resonance of an array of SRRs is also determined by the refractive index of the substrate supporting the SRR patterns [15,16]. The SRRs fabricated on lower refractive index materials (e.g. silica) characteristically show their LC resonant response at higher frequencies than those fabricated on silicon. Figure 2 shows that the aluminium SRRs fabricated on silicon display an LC peak in the wavelength region around 930 nm. By keeping the dimensions and all other parameters of the smaller SRRs of Fig. 2. constant, but changing the substrate to silica, it is possible to shift the LC response to even shorter wavelengths. So, by fabricating very small aluminium based SRRs on silica substrates, it is possible to obtain an LC resonant response at visible wavelengths. Figure 4 shows results for different sized Au and Al SRRs fabricated on silica, displaying LC peaks in the visible part of the spectrum.

As shown in Fig. 4. the aluminium based SRRs of dimensions ($l/3$) varies from ~150 nm to ~100 nm fabricated on silica, displays the LC resonance between 680 nm to as low as 530 nm wavelengths, well inside the visible spectrum region. Whereas the smallest dimension ($l/3$) of ~100 nm gold based SRRs fabricated on silica displays the LC peak at 720 nm, just on the edge of the visible spectrum. This clearly demonstrates the advantage of aluminium based SRRs in pushing the magnetic resonance (LC resonance) to higher frequency visible spectrum when compared with their gold based counterparts.

Small Al SRRs on Silica Substrate



Small Au SRRs on Silica Substrate

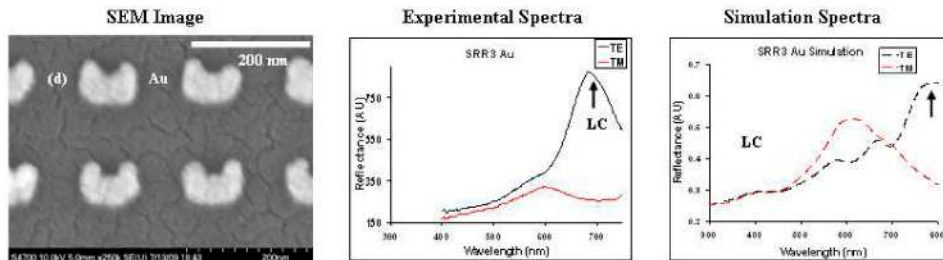


Fig. 4. Table showing the reflectance spectra of the different SRR patterns fabricated on silica. The first three rows are small sized (~150 to 120 nm) aluminium SRRs with (a) SRR 3 Al (b) SRR 4 Al and (c) SRR 5 Al and the last row is small sized (~120 nm) gold SRR with (d) SRR 3 Au along with their corresponding experimental (solid curves) and simulation (dashed curves) spectra. Black curves (solid and dashed) are TE and Red curves (solid and dashed) are TM measurements.

In Fig. 5. we display TE field plots of SRR 4-Al at both the plasmonic and LC resonant peaks.

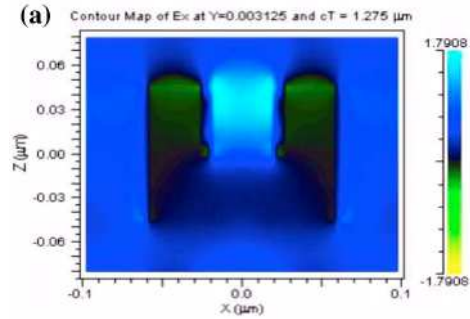


Fig. 5. (a) Field profile of SRR-4 Al at the plasmonic resonance peak (370 nm)

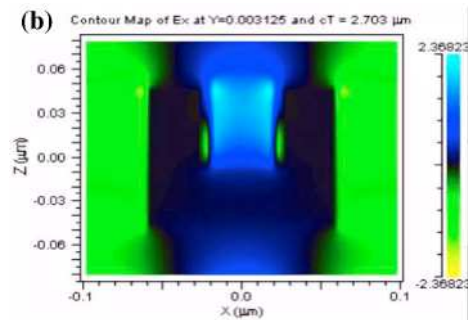


Fig. 5. (b) Field profile of SRR-4 Al at the LC resonance peak (670 nm)

Figure 5 clearly shows the different distributions of the optical electric field for the two different resonances. In the case of the plasmon resonance, the phase and amplitude of the optical electric field has a uniform distribution around the SRR structure - and it is in phase with the field in the gap of the SRRs. The LC resonance on the other hand exhibits a completely different situation, in which the optical electric field between the arms of the SRRs is in anti-phase with the light on either side of the SRR structure. From this difference in behaviour, it may be inferred that the LC resonance condition is a fundamentally different one from the plasmonic resonance condition. Our description of the resonance behaviour therefore differs from that of reference [6], but is consistent with that of Linden et al [3].

8. Conclusion

We have shown that, at higher frequencies, both the dimensions and the individual metal properties play an important role in determining the resonant response of arrays of SRRs. In particular, we have shown that the use of aluminium, due to its bulk plasma frequency being higher than that of gold, enables a large shift of the magnetic response towards shorter wavelengths. Finally, we have utilised this property of aluminium and have fabricated aluminium-based SRRs on low refractive index substrates, i.e. silica, to demonstrate clear magnetic resonances of SRRs at visible frequencies as short as 530 nm.

Acknowledgements

The authors wish to acknowledge support from the European Commission through the Metamorphose NoE, ECONAM and COST action MP0702 - and also the staff and facilities of the James Watt Nanofabrication Centre at Glasgow University.